Research Article

EASL EUROPEAN ASSOCIATION FOR THE STUDY OF THE LIVER | JOURNAL OF HEPATOLOGY

Structural and inflammatory heterogeneity in subcutaneous adipose tissue: Relation with liver histopathology in morbid obesity

Joan Tordjman[1,2,*], Adeline Divoux[2], Edi Prifti[2], Christine Poitou[1,2,3], Veronique Pelloux[1,2], Danielle Hugol[4], Arnaud Basdevant[1,2,3], Jean-Luc Bouillot[5], Jean-Marc Chevallier[6], Pierre Bedossa[7], Michèle Guerre-Millo[1,2], Karine Clement[1,2,3]

[1]*ICAN Institut Cardiométabolisme et Nutrition, Paris, Pitié-Salpêtrière Hospital, Paris F-75013, France;* [2]*INSERM, U872, Nutriomique, Paris F-75006, France; Université Pierre et Marie Curie-Paris6, Centre de Recherche des Cordeliers, UMR S 872, Paris F-75006, France;* [3]*CRNH-Ile de France, Paris F-75013, France;* [4]*Assistance Publique-Hôpitaux de Paris, Hôtel-Dieu Hospital, Anatomo-pathology Department, Paris F-75004, France;* [5]*Assistance Publique-Hôpitaux de Paris, Hôtel-Dieu Hospital, Surgery Department, Paris F-75004, France;* [6]*Assistance Publique-Hôpitaux de Paris, Hôpital Européen Georges Pompidou, Diabetology-Edocrinology-Nutrition Department, Paris, France;* [7]*Assistance Publique-Hôpitaux de Paris, Beaujon Hospital, Pathology Department, Clichy F-92110, France; Centre de Recherche Bichat-Beaujon, INSERM U773, Clichy F-92110, France*

Background & Aims: In addition to total body fat, the regional distribution and inflammatory status of enlarged adipose tissue are strongly associated with metabolic co-morbidities of obesity. We recently showed that the severity of histological liver lesions related to obesity increases with the amount of macrophage accumulation in visceral adipose tissue (VAT), while no association was found with the subcutaneous adipose tissue (SAT). In the abdominal region, SAT is anatomically divided into two layers, i.e. superficial (sSAT) and deep (dSAT). The aim of the present study was to test the hypothesis that these distinct compartments differentially contribute to hepatic alterations in obesity.

Methods: Biopsies of the liver, sSAT, dSAT, and VAT were collected in 45 subjects with morbid obesity (age 43.7 ± 1.6 years; BMI 48.5 ± 1.2 kg/m^2) during bariatric surgery. Large scale gene expression analysis was performed to identify the pathways that discriminate sSAT from dSAT. Adipose tissue macrophages were quantified by immunohistochemistry using HAM56 antibody in subjects scored for liver histopathology.

Results: An inflammatory gene pattern discriminates between sSAT and dSAT. dSAT displayed an intermediate level of macrophage accumulation between sSAT and VAT. The abundance of macrophages in dSAT, but not in sSAT, was significantly increased in patients with non-alcoholic steatohepatitis (NASH) and/or fibroinflammatory hepatic lesions.

Conclusions: These data show distinct gene signature and macrophage abundance in the two compartments of SAT, with dSAT more closely related to VAT than to sSAT in terms of inflammation and relation with the severity of liver diseases in morbid obesity.

Keywords: Bile acids; Cholestasis; Fatty liver disease; Gallstones; Liver regeneration; Liver cancer.

Received 20 June 2011; received in revised form 6 December 2011; accepted 7 December 2011; available online 13 January 2012

* Corresponding author. Address: Centre de Recherche des Cordeliers, UMR S 872, Team 7, 15 rue de l'Ecole de Médecine, Paris F-75006, France. Tel.: +33 142346956; fax: +33 142346993.

E-mail address: joan.tordjman@crc.jussieu.fr (J. Tordjman).

Abbreviations: NAFLD, non-alcoholic fatty liver disease; VAT, visceral adipose tissue; SAT, subcutaneous adipose tissue; sSAT, superficial SAT; dSAT, deep SAT; NASH, non-alcoholic steatohepatitis; QUICKI, quantitative insulin sensitivity check index; CSF3, colony-stimulating factor 3; IL-6, interleukin 6; CXCL, C-X-C motifs chemokines; PLAUR, plasminogen activator urokinase receptor; SOCS3, suppressor of cytokine signaling 3.

Introduction

Obesity-associated co-morbidities include alteration of glucose homeostasis, increased cardio-vascular risks and non-alcoholic liver diseases (NAFLD). There is a wealth of epidemiological and clinical evidence indicating that both total body fat accumulation and regional distribution of enlarged adipose tissue contribute to obesity complications [1]. A putative link between increasing fat mass and ensuing complications is the low-grade inflammatory state that prevails in adipose tissue and is characterized by macrophage accumulation. We and others have shown that the abundance of adipose tissue macrophages differs among fat depots. There are twice as many macrophages in visceral adipose tissue (VAT) than in subcutaneous adipose tissue (SAT) [2,3]. Through the release of pro-inflammatory mediators, macrophages might account, at least in part, for the association between increased VAT mass and co-morbidities associated with central obesity [1]. We previously showed the association between increased accumulation of macrophages in VAT and high grades of steatosis and/or high index of fibro-inflammation in the liver of obese subjects [4]. In marked contrast, no association was evidenced between the severity of liver histopathology and macrophage counts in SAT sampled superficially in the abdominal region. At first sight, this finding would diminish the impact of the pathophysiological alterations of SAT in the complications of human obesity such as liver diseases. However, abdominal SAT is anatomically separated by a fascial plane into superficial (sSAT)

Table 1. Clinical and biological parameters of 45 morbidly obese subjects.

			No NASH	NASH
	n	45	28	10
	Gender F/M (n)	36/9	24/4	7/3
	Age (yr)	43.73 ± 1.58	43.23 ± 1.93	46.90 ± 3.11
	BMI (kg/m^2)	48.49 ± 1.19	47.93 ± 1.51	49.90 ± 2.52
Glycemic parameters	Glucose (mM)	6.27 ± 0.29	6.11 ± 0.38	6.99 ± 0.64
	Insulin (μU/ml)	19.55 ± 2.44	18.59 ± 3.19	25.34 ± 5.15
	QUICKI	0.312	0.31	0.30
	Diabetics	37.7%	32.1%	60%*
Lipid parameters	Cholesterol (mM)	4.81 ± 0.21	4.69 ± 0.28	5.23 ± 0.49
	HDL-cholesterol (mM)	1.17 ± 0.05	1.13 ± 0.06	1.16 ± 0.10
	ApoA1 (mM)	1.23 ± 0.04	1.20 ± 0.05	1.26 ± 0.08
	Triglycerides (mM)	1.89 ± 0.42	2.05 ± 0.57	1.66 ± 0.96
Inflammatory parameters	Leptin (ng/ml)	59.02 ± 4.31	63.08 ± 5.68	56.30 ± 8.81
	Adiponectin (μg/ml)	8.85 ± 1.15	9.22 ± 1.06	5.22 ± 1.79§
	IL-6 (pg/ml)	4.32 ± 0.21	4.43 ± 0.68	4.29 ± 1.15
	hsCRP (mg/dl)	9.48 ± 1.37	8.77 ± 1.69	11.35 ± 2.72
Hepatic factors	AST (IU/L)	26 ± 2	24 ± 3	29 ± 4
	ALT (IU/L)	35 ± 3	38 ± 4	44 ± 7
	γGT (mg/dl)	55 ± 11	50 ± 14	86 ± 25

Means ± SEM are given.
AST, aspartate aminotransferase; ALT, alanine aminotransferase; γGT, γ-glutamyltransferase.
*$p < 0.01$.
§$p < 0.05$.

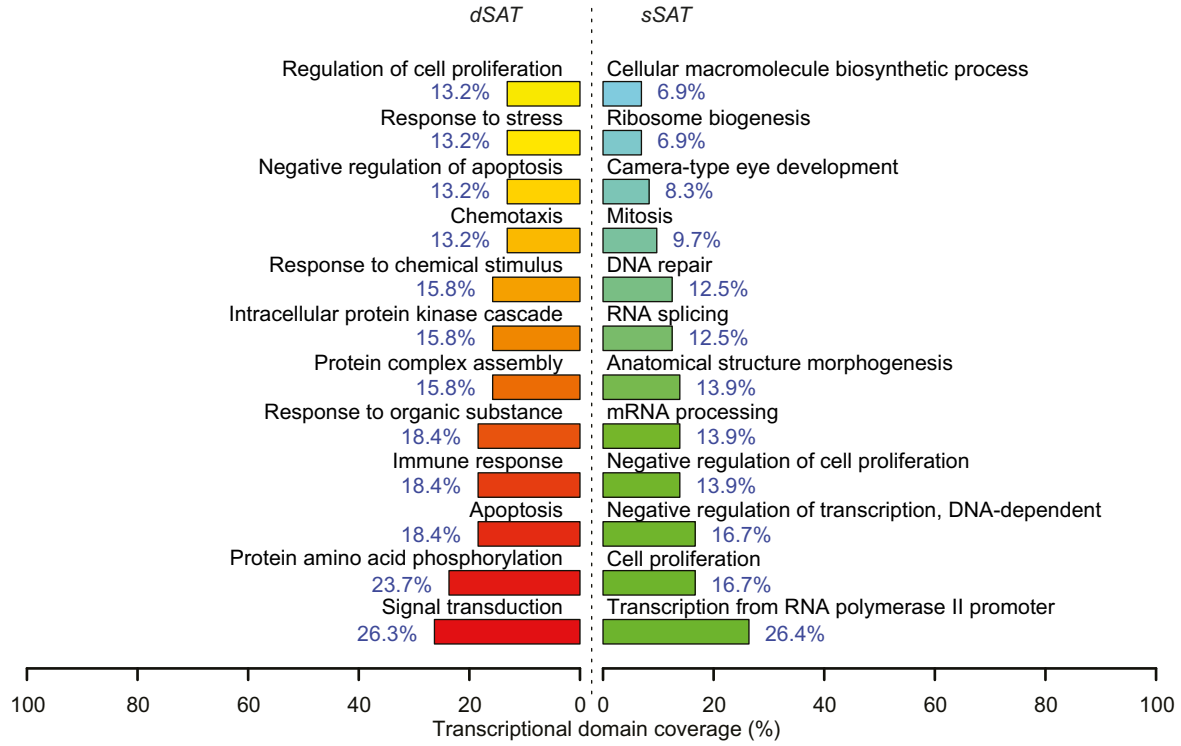

Fig. 1. Functional signature of the difference between dSAT and sSAT at the transcriptomic level. Functional themes represented by enriched annotating categories of Gene Ontology biological process at the specificity level 6. (This figure appears in color on the web).

Table 2. List of the up-regulated genes in dSAT included in the human proteome dataset.

Gene ID #	Name	Symbol	Fold change
950	Scavenger receptor class B, member 2	*SCARB2*	1.28
51088	Kelch-like 5 (*D. melanogaster*)	*KLHL5*	1.29
3122	Major histocompatibility complex, class II, DR alpha	*HLA-DRA*	1.30
8743	Tumor necrosis factor (ligand) superfamily, member 10	*TNFSF10*	1.31
51088	Kelch-like 5 (*D. melanogaster*)	*KLHL5*	1.32
6892	TAP binding protein (tapasin)	*TAPBP*	1.40
1827	Regulator of calcineurin 1	*RCAN1*	1.47
1839	Heparin-binding EGF-like growth factor	*HBEGF*	1.53
5329	Plasminogen activator, urokinase receptor	*PLAUR*	1.57
6400	Sel-1 suppressor of lin-12-like (*C. elegans*)	*SEL1L*	1.57
6515	Solute carrier family 2 (facilitated glucose transporter), member 3	*SLC2A3*	1.63
1282	Collagen, type IV, alpha 1	*COL4A1*	1.66
2081	Endoplasmic reticulum to nucleus signaling 1	*ERN1*	1.76
2921	Chemokine (C-X-C motif) ligand 3	*CXCL3*	1.85
7057	Thrombospondin 1	*THBS1*	1.93
6355	Chemokine (C-C motif) ligand 8	*CCL8*	1.97
3491	Cysteine-rich, angiogenic inducer, 61	*CYR61*	1.98
2920	Chemokine (C-X-C motif) ligand 2	*CXCL2*	2.11
3569	Interleukin 6 (interferon, beta 2)	*IL6*	2.28
1440	Colony stimulating factor 3 (granulocyte)	*CSF3*	2.47

and deep subcutaneous adipose tissue (dSAT). A few studies, in which fat accumulation was measured by computed tomography (CT), have shown strong links between both VAT and dSAT and blood parameters of insulin resistance and dyslipidemia, while association with sSAT was much weaker [5,6]. This could rely on differences in gene expression, with dSAT reflecting more a VAT expression profile than sSAT, as shown for a limited number of genes [7,8].

The potential distinct implication of dSAT versus sSAT in the alteration of glucose and lipid homeostasis prompted us to investigate a depot-specific relationship with liver pathology in obesity. We performed large scale gene expression analysis to identify the pathways that discriminate sSAT from dSAT and quantified the amounts of macrophages in obese subjects scored for liver histopathology.

Materials and methods

Human subjects

The study enrolled 45 obese subjects involved in a gastric surgery program and recruited between 2002 and 2006 at the Department of Nutrition of Hôtel-Dieu Hospital (Paris, France), as described in detail elsewhere [9]. Briefly, the subjects met the criteria for obesity surgery, i.e. body mass index (BMI) $\geqslant$40 or $\geqslant$35 kg/m^2 with at least one significant co-morbidity. They all underwent a gastric bypass surgery. A careful report of the subjects' personal history of body weight changes was collected. The subjects were weight stable during the 3 months prior to surgery. Subjects were excluded if they had evidence of autoimmune, inflammatory or infectious diseases, including viral hepatitis, cancer, known alcohol consumption (>20 g/day), or kidney diseases. Seventeen subjects (37.7% of the initial population) were considered to be type 2 diabetic subjects (T2D) according to the criteria of fasting glycemia over 7 mM or treatment. Among them, 4 were not treated, 10 were treated with metformin, 3 with insulin, and 7 with hypolipemic drugs (fibrates or statins). Paired superficial, deep subcutaneous and visceral (omental) adipose tissue surgical biopsies and a needle liver biopsy were obtained from all subjects at the time of gastric surgery. The Ethics Committees of the Hôtel-Dieu Hospital approved the clinical investigations and all subjects signed a written informed consent prior to their inclusion in the study. Clinical and biological parameters of the participants are shown in Table 1.

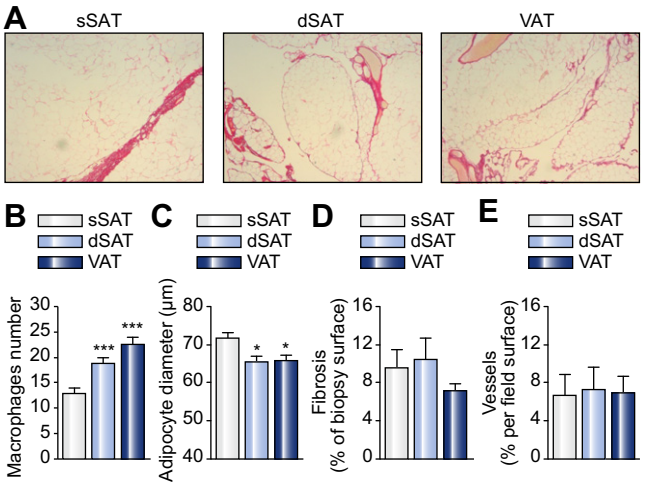

Fig. 2. Morphological and cellular aspects of sSAT, dSAT, and VAT in obesity. (A) Morphological aspect of sSAT, dSAT, and VAT observed after hematoxylin/eosin staining in 10× magnification; (B) HAM56 positive macrophage accumulation (n = 45); (C) adipocyte diameters (n = 45); (D) fibrosis amounts (n = 11); and (E) vessel density (n = 11) in sSAT, dSAT, and VAT biopsies obtained in obese subjects at the time of gastric surgery. Data are expressed as mean ± SEM. $^{***}p$ <0.0001, $^{*}p$ <0.05 compared to sSAT values. (This figure appears in color on the web).

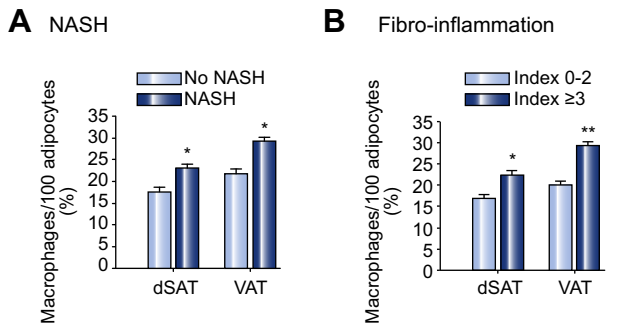

Fig. 3. Liver histopathology and adipose tissue macrophages. Number of HAM56 positive macrophages in dSAT and VAT in 38 subjects scored for (A) hepatic NASH and (B) fibroinflammation. $^{*}p$ <0.05, $^{**}p$ <0.001 compared to no NASH or index 0–2.

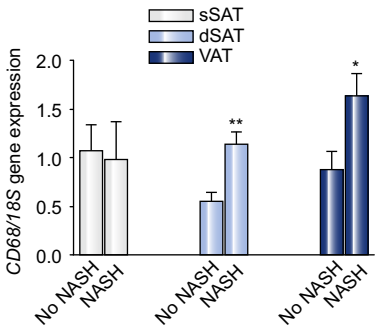

Fig. 4. Liver histopathology and *CD68* gene expression in sSAT, dSAT, and VAT. *CD68* gene expression was determined by qRT-PCR analysis in paired sSAT, dSAT, and VAT biopsies obtained in 38 obese subjects. $^{*}p$ <0.05, $^{**}p$ <0.001 compared to no NASH.

Table 3. Liver characteristics of the 38 morbidly obese subjects.

Liver histopathology		n = 38
Steatosis	score 0, 1	16 (42%)
	score ≥2	22 (58%)
Fibrosis	stage F0, F1	23 (60.5%)
	stage F2, F3	15 (39.5%)
Portal inflammation	score 0	19 (50%)
	score 1	19 (50%)
Lobular inflammation	Score 0-1	34 (89.5%)
	Score 2-3	4 (9.5%)
NAS	0-2	15 (39.5%)
	3-4	13 (34.2%)
	≥5 (NASH)	10 (26.3%)
Fibro-inflammation	index 0-2	23 (60.5%)
	index ≥3	15 (39.5%)

The data are shown as number of subjects (percent of total). Liver histopathology was scored as indicated in Materials and methods.
BMI, body mass index; NAS, NAFLD activity score; NASH, non-alcoholic steatohepatitis.

Liver histopathology

Among the 45 subjects, 38 underwent liver biopsies that were scored and analyzed by a single expert pathologist. Major histopathological features were semi-quantified according to previously published criteria [10,11]. The amount of steatosis, defined as the percentage of hepatocytes with fat droplets, was scored using the following scale: 0 (0–5%), 1 (5–33%), 2 (34–66%) and 3 (>67%). Foci of lobular inflammation were defined as 2 or more inflammatory cells (averaged from 3 to 4 fields) counted at 20× magnification and then classified as 0 (none), 1 (<2 foci) and 2 (2–4 foci). Portal inflammation was evaluated by inflammatory infiltrates assessed at low magnification and scored 0 (no or rare inflammatory cells), 1 (few aggregates of inflammatory cells) and 2 (densely packed inflammatory cells). Fibrosis was scored according to Brunt [10], as stage 0 (F0: none), stage 1 (F1: zone 3 perisinusoidal or portal fibrosis), stage 2 (F2: zone 3 perisinusoidal and periportal fibrosis without bridging), stage 3 (F3: bridging fibrosis), stage 4 (F4: cirrhosis). Hepatocyte ballooning was scored as 0 (none), 1 (few) or 2 (many). Absence or presence of NASH (non-alcoholic steatohepatitis) was evaluated according to standard histopathologic criteria and severity of the disease was assessed using the NAS (non-alcoholic fatty liver disease activity score) established by Kleiner *et al.* [11] as the unweighted sum of scores of steatosis, lobular inflammation and hepatocellular ballooning. NASH was considered as diagnostic for NAS ⩾5. Although a recent report suggests that selection based on a NAS score >5 may include few cases that would not meet all criteria for NASH [12], we reviewed in the present study all cases selected through a NAS score ⩾5 to ensure that they all display steatosis, ballooning of hepatocyte and lobular inflammation with a predominance in zone 3. In order to independently assess the severity of chronic inflammation independently of steatosis, we used a fibro-inflammation index described elsewhere [2]. This index is the unweighted sum of elementary scores of fibrosis, portal inflammation and lobular inflammation [2]. To grade the participants according to the type and severity of liver damage, we used both the score of NAS and our created index of fibro-inflammation.

Laboratory tests

Blood samples were collected after an overnight fast. Plasma glucose, triglycerides, total cholesterol and HDL-cholesterol levels were immediately measured enzymatically. Serum insulin concentrations were determined with an IRMA kit (Bi-INSULIN IRMA CisBio International, Gif-sur-Yvette, France). Insulin sensitivity was evaluated by the quantitative insulin sensitivity check index [13]: QUICKI = 1/[log fasting insulin (mU/L) + log fasting glycemia (mg/dl)]. Serum leptin and adiponectin were determined using radioimmunoassay kits (Linco Research, Saint Louis, MI, USA). Interleukin 6 (IL-6) serum levels were measured by an ultrasensitive ELISA system (QuantikineUS, R&D System Europe Ltd., Abingdon, UK). Using these assays, the values found in 30 lean healthy subjects are: leptin: 14.6 ± 1.75 ng/ml, adiponectin: 15.3 ± 2.02 μg/ml and IL-6: 2.3 ± 0.5 pg/ml.

mRNA amplification and microarrays

Eight patients were considered for microarray experiments. Clinical and biological characteristics of this subjects' subset were similar to the entire group (Supplementary Table 1). Total RNA from sSAT and dSAT was prepared using the RNeasy total RNA Mini kit (Qiagen, Courtaboeuf, France), following the manufacturer's protocol. The concentration of total RNA was determined using Ultrospec 2000 spectrophotometer (Pharmacia Biotech, Piscataway, NJ, USA) and the RNA integrity was assessed using a 2100 Bioanalyzer (Agilent Technologies, Massy, France). One microgram of total RNA from each sample was amplified with the MessageAmp RNA kit (Ambion, Austin, TX), and 3 μg of amplified RNA (aRNA) was Cy-dye labeled using the CyScribe first-strand cDNA labeling kit (Amersham Biosciences, Orsay, France). dSAT aRNAs were labeled with Cy-5 (red) and sSAT aRNAs with Cy-3 (green). Following a type-I design, the samples were hybridized on Agilent 4× 44K whole human genome microarrays. Sample preparation, hybridization, and microarray washing were performed according to manufacturer's recommendations (Agilent Technologies, Massy, France).

Microarray data analysis

Raw data were extracted with Scanning (GenePix 4000A Scanner Axon Instruments-Molecular Devices, Sunnyvale, CA) using default settings. Data were normalized in the R statistical environment using the 'limma' package [14,15]. A 'lowess' within-array and 'quantile' inter-array normalization was performed without background correction. Normalized data were filtered and only those genes with valid expression measurements for at least 80% of the samples were considered. The raw microarray data are available for download at the Gene Expression Omnibus (GEO) public repository (access link number: GSE30133).

We used SAM software (Significance Analysis of Microarray) with a 'one class' option to identify genes whose expression was discriminated between dSAT and sSAT [16]. Only genes with false discovery rate (FDR) smaller than 5% were

retained for further analyses. The functional exploration of the differentially expressed genes consisted of three main steps: (i) identification of relevant biological annotations representing the contextual transcriptomic signature, (ii) construction and analysis of the gene co-expression network, and (iii) based on the two previous steps, construction of functional interaction maps that characterize the transcriptomic signature.

An automated annotation procedure of the differentially expressed genes was performed with the FunNet tool using a two-list non-discriminant analysis and Gene Ontology annotation database, as described in [17,18]. The analytical framework used to construct the co-expression network was based on previous work by Zhang and Horvath [19]. Spearman's correlation coefficient was used to quantify the similarity between gene expression profiles and produce a co-expression matrix. Next, a "hard" threshold of 0.9 was applied to the latter in order to obtain an adjacency matrix, which represents the final network. This threshold value was determined by maximizing a scale-free topology criterion as previously described [19]. A comprehensive map illustrating the interactions between biological themes, which characterize the transcriptomic signature of the differentially expressed genes, was obtained with the FunNet tool using a two-list non-discriminant analysis.

Predicting secreted factors

Protein accession numbers were obtained for up and down expressed genes in dSAT to use TargetP [20] and SecretomeP [21] programs. Only genes coding for proteins that were identified as "secreted" by TargetP were considered in this analysis. Crossing the list with the non-redundant list of 1175 proteins identified in plasma (Human Proteome dataset) compiled by Anderson *et al.* [22] allowed to identify SAT genes coding for proteins present in the circulation.

Adipose tissue histopathology

For all patients, paired biopsies of omental, superficial and deep subcutaneous adipose tissue were processed and embedded in paraffin. Sections of 5 μm were stained with hematoxylin/eosin for adipocyte diameter determination using PerfectImage Software (Claravision, France). Macrophages were detected using HAM56 antibody (Dako Cytomation, Trappes, France). Slides were observed under a Zeiss 20 Axiostar Plus microscope (Zeiss, Germany) and digital images were captured by a camera (triCCD, Sony, France). Adipocytes and HAM56+ cells were counted in 10 different randomly chosen areas, at 40× magnification. Three independent observers blindly performed the counting and values were averaged. The number of HAM56+ cells per 100 adipocytes is considered the number of infiltrating adipose tissue macrophages. To perform fibrosis quantification, slides of adipose tissue biopsies were stained with picrosirius red. Fibrosis analysis was performed with histomorphometry using Alphelys platform (Histolab software, Plaisir, France) at 100× magnification with content color thresholds. The quantification of total fibrosis was expressed as the ratio of fibrous tissue area as stained with picrosirius red staining/total tissue surface as described [17]. The vascular density was measured on slides stained with anti-Von Willebrand factor antibody (1:200, Dako, Trappes, France). Vessel labeling was measured in five fields per biopsy at 10× magnification. To quantify vascular density, Von Willebrand labeled surface was normalized to field surface and expressed in percent.

Statistical analyses

Data are expressed as mean ± SEM. The Shapiro–Wilks test was used to test the Gaussian distribution of biological parameters. Skewed variables were log-transformed to normalize their distribution before statistical analyses. Student's *t* test was used for comparison between groups. Statistical analyses were performed with JMP statistics software (SAS Institute Inc., Cary, NC, USA) or GraphPad Prism version 3.00 for Windows (GraphPad Software, San Diego, CA, USA). A p value <0.05 was considered as significant.

Results

Transcriptomic signature of dSAT

To gain insight into the signaling pathways and biological processes that discriminate the two compartments of SAT, we examined the transcriptomic signature of 8 paired dSAT and sSAT biopsies obtained in obese subjects during gastric surgery. Following the filtering procedure, the expression profiles of 21,716 genes were retained for the differential expression analysis. Using a 5% false discovery rate, we detected 97 cDNAs up-regulated (fold-change: 1.22–2.47) and 385 cDNA down-regulated (fold-change: 0.87–0.55) in dSAT as compared to sSAT (Supplementary Tables 2 and 3). Genes whose expression changed between dSAT and sSAT were grouped with the GO Biological Process annotations at specificity level 6 (Fig. 1). Over-represented biological processes in dSAT included "response to stress", "chemotaxis", "immune response" and "signal transduction". Among the most differentially expressed genes, a number of genes related to inflammation were up-regulated in dSAT, including colony-stimulating factor 3 (*CSF3*), interleukin 6 (*IL-6*), several C-X-C and C-C motifs chemokines, the plasminogen activator urokinase receptor (*PLAUR*) and suppressor of cytokine signaling 3 (*SOCS3*). Looking for potentially secreted proteins, we found that 20 out of the 97 genes overexpressed in dSAT coded for proteins listed in the human plasma proteome dataset (Table 2), including a number of inflammatory factors (CSF3, IL-6, CXCL2, CCL8, CXCL3, PLAUR). These data identify the transcriptomic signature of dSAT characterized by an overexpression of genes coding for inflammation-related secreted factors, as compared to sSAT. Supplementary Fig. 1 illustrates the modular organization and the relations between the functional themes that characterize the genomic signature of dSAT, based on gene expression profile.

Morphological aspect and macrophage counts in dSAT

A distinct morphological aspect of sSAT, dSAT, and VAT was observed in hematoxylin–eosin stained adipose tissue slides. dSAT displayed a lobule-like structure similar to that observed in VAT and clearly distinct from the more homogenous aspect of sSAT (Fig. 2A). Measure of adipocyte diameter in the three depots revealed larger adipocytes in sSAT (71.8 ± 1.31 μm) than in dSAT (65.4 ± 1.38 μm, $p = 0.027$) and in VAT (65.7 ± 1.58 μm, $p = 0.029$) (Fig. 2B). The number of HAM56+ cells normalized to 100 adipocytes showed a graded increase from sSAT (12.9 ± 0.99) to VAT (22.6 ± 1.48), with dSAT exhibiting an intermediate level (18.8 ± 1.19) significantly higher than in sSAT ($p < 0.0001$) and not significantly different ($p = 0.052$) from VAT (Fig. 2C). By contrast, the amount of fibrosis (Fig. 2D) and vessels (Fig. 2E) was similar in the three depots. Thus, the dSAT of obese subjects appears to have greater similarities with VAT than with sSAT, with regards to morphology, adipocyte size and macrophage accumulation.

dSAT macrophages and liver histopathology

The inflammatory expression profile and increased macrophage content in dSAT prompted us to evaluate the potential impact on liver histopathology. We performed a detailed semi-quantitative histological analysis of liver biopsies in 38 obese subjects included in the initial population. sSAT, dSAT, and VAT macrophage number was determined in subjects separated into two groups with a distinct degree of severity according to absence (n = 28) or presence of NASH (n = 10) and to fibro-inflammation index lower (n = 23) or higher (n = 15) than 3 (Table 3). Whatever the category of liver histopathology, the subjects with the severest alterations had systematically higher numbers of macrophage in both dSAT and VAT than those with milder or no alterations

(Fig. 3). No significant difference was found in sSAT macrophage count between the groups with severe or mild/absent histopathology (data not shown).

Discussion

This study shows that abdominal SAT of morbidly obese subjects is not homogenous in terms of morphology and inflammatory status. dSAT appears more related to VAT than to sSAT with regards to lobular organization and adipose cell size, while vessel density and the amount of fibrosis were similar in the three depots. Striking differences between dSAT and sSAT arose from large-scale exploration of gene signature, showing that genes related to inflammation clearly discriminate the two depots. Many of the overexpressed genes in dSAT were secreted inflammatory factors, potentially produced by a higher number of macrophages than in sSAT. In accordance with this possibility, the number of macrophages quantified by immunohistochemistry was higher in dSAT and VAT than in sSAT. Importantly, patients with NASH and/or severe fibroinflammation displayed more macrophages in both dSAT and VAT than subjects without liver alterations. Low tissue availability in this study limited the validation of microarray data at the level of gene or protein expression. Notwithstanding this limitation, we measured the gene expression of a pan-macrophage marker CD68 and found increased expression in dSAT and VAT in patients with NASH. Although these data do not represent a cause and effect proof, they suggest a link between liver histopathology and macrophage infiltration in specific fat depots. Nevertheless, we cannot exclude the contribution of other immune cells, including T-lymphocytes [23] and mast cells [24] that were recently shown to accumulate in adipose tissue in human obesity (Fig. 4).

When measured by CT scan, SAT represents a significant amount of fat mass in the abdominal region, with a roughly similar contribution of the two compartments [5,6]. Thus, production of inflammatory factors by dSAT might account substantially for systemic low-grade inflammation in human obesity. Moreover, the amount of dSAT has been associated with insulin resistance in lean and moderately obese subjects [5,6]. Currently, it is not clear whether this relies on increased inflammation and macrophage content in this depot. The inverse correlation of SAT expression of the macrophage marker CD68 and whole body insulin sensitivity [25,26] and the increased number of macrophage crown-like structures in SAT of insulin resistant obese subjects [27] argue for a role of SAT inflammation in insulin resistance. In morbidly obese subjects however, we did not found any significant association between blood-derived glycemic parameters and adipose tissue macrophage counts in SAT or VAT [2,28,29]. This was confirmed in the current study, where macrophages accumulation in sSAT, dSAT or VAT did not correlate significantly with serum insulin, serum glucose or QUICKI values (data not show). This leaves open the question of the mechanisms linking increased dSAT mass to insulin resistance in human obesity.

In general, the deep layer of subcutaneous adipose tissue displays characteristics that reflect more those of the visceral adipose tissue than those of the superficial layer of subcutaneous adipose tissue. This is substantiated by immunohistological exploration, which showed similar adipocyte size and macrophage content in dSAT and VAT, clearly distinct from sSAT. The close similarities in macrophage accumulation between dSAT and VAT and the increased inflammatory status of dSAT as compared to sSAT raised the hypothesis of a link with liver histopathology. We confirmed here the association between VAT macrophages and severe liver pathology (NASH and high fibroinflammation) [4,30] and extend this relationship to dSAT. This reinforces the proximity between dSAT and VAT for advanced stages of liver injury in obesity.

Increased free fatty acid fluxes and/or delivery of macrophage-derived pro-inflammatory factors to the liver *via* the portal circulation have been proposed as molecular links between VAT and liver alterations [31]. To what extent inflammatory factors released from dSAT macrophages also contribute to increase delivery of deleterious factors into the liver remains to be evaluated. We probably need more information on the vascularization networks potentially different in dSAT and sSAT. Nevertheless, the inflammatory factors, identified in the present study as overexpressed in dSAT, represent potential candidate biomarkers that could impact on liver injury. Some of them, mostly interleukins such as IL-6 measured in the circulation, have been associated with liver alterations. It could be worth testing other mediators described here such as CXCL chemokines or plasminogen activator, urokinase receptor (PLAUR) in larger cohorts of subjects in whom liver histopathology is known. Interestingly, we showed recently that PLAUR is selectively overexpressed in macrophages that infiltrate adipose tissue in obese subjects and we observed that its circulating levels were associated with markers of insulin sensitivity [32]. The plasminogen-activating system has been involved in liver injury such as fibrosis or cancer [33,34]. Whether components of this system produced by dSAT could contribute to aggravated stages of liver alteration in obesity may deserve future consideration.

Our study shows that sSAT and dSAT are distinct depots in accordance with the anatomical separation of the fascia superficialis and opens the interest for a deeper investigation of dSAT as an indicator of liver alterations. This could represent a clinical advantage to evaluate liver damages in morbidly obese subjects. Further studies are required to elucidate physiological differences in dSAT, sSAT, and VAT, which may provide insight into the mechanisms of NAFLD during obesity.

Conflict of interest

The authors who have taken part in this study declared that they do not have anything to disclose regarding funding or conflict of interest with respect to this manuscript.

Financial Support

This work was supported by the « Programme Hospitalier de Recherche Clinique », Assistance Publique-Hôpitaux de Paris (AOR 02076) and by the Commission of the European Communities (Collaborative Project "Hepatic and adipose tissue and functions in the metabolic syndrome" HEPADIP, see http://www.hepadip.org/, contract LSHM-CT-2005-018734). The research leading to these results has received funding from the European Union Seventh Framework Programme (FP7/2007-2013) under grant agreement no Health-F2-2009-241762, for the project FLIP. We also thank for their individual support the

"Fondation pour la Recherche Médicale" (to AD), and the CODDIM (to KC and MGM).

Acknowledgments

We thank Florence Marchelli and Christine Baudouin who contributed to the database constitution and Patricia Bonjour for her help with histochemistry.

Supplementary data

Supplementary data associated with this article can be found, in the online version, at doi:10.1016/j.jhep.2011.12.015.

References

[1] Lafontan M, Girard J. Impact of visceral adipose tissue on liver metabolism. Part I: heterogeneity of adipose tissue and functional properties of visceral adipose tissue. Diabetes Metab 2008;34:317–327.
[2] Cancello R, Tordjman J, Poitou C, Guilhem G, Bouillot JL, Hugol D, et al. Increased infiltration of macrophages in omental adipose tissue is associated with marked hepatic lesions in morbid human obesity. Diabetes 2006;55:1554–1561.
[3] Harman-Boehm I, Bluher M, Redel H, Sion-Vardy N, Ovadia S, Avinoach E, et al. Macrophage infiltration into omental versus subcutaneous fat across different populations: effect of regional adiposity and the comorbidities of obesity. J Clin Endocrinol Metab 2007;92:2240–2247.
[4] Tordjman J, Poitou C, Hugol D, Bouillot JL, Basdevant A, Bedossa P, et al. Association between omental adipose tissue macrophages and liver histopathology in morbid obesity: influence of glycemic status. J Hepatol 2009;51:354–362.
[5] Smith SR, Lovejoy JC, Greenway F, Ryan D, DeJonge L, de la Bretonne J, et al. Contributions of total body fat, abdominal subcutaneous adipose tissue compartments, and visceral adipose tissue to the metabolic complications of obesity. Metabolism 2001;50:425–435.
[6] Kelley DE, Thaete FL, Troost F, Huwe T, Goodpaster BH. Subdivisions of subcutaneous abdominal adipose tissue and insulin resistance. Am J Physiol Endocrinol Metab 2000;278:E941–E948.
[7] Walker GE, Verti B, Marzullo P, Savia G, Mencarelli M, Zurleni F, et al. Deep subcutaneous adipose tissue: a distinct abdominal adipose depot. Obesity (Silver Spring) 2007;15:1933–1943.
[8] Alvehus M, Buren J, Sjostrom M, Goedecke J, Olsson T. The human visceral fat depot has a unique inflammatory profile. Obesity (Silver Spring) 2010;18:879–883.
[9] Poitou C, Coupaye M, Laaban JP, Coussieu C, Bedel JF, Bouillot JL, et al. Serum amyloid A and obstructive sleep apnea syndrome before and after surgically-induced weight loss in morbidly obese subjects. Obes Surg 2006;16:1475–1481.
[10] Brunt EM, Janney CG, Di Bisceglie AM, Neuschwander-Tetri BA, Bacon BR. Nonalcoholic steatohepatitis: a proposal for grading and staging the histological lesions. Am J Gastroenterol 1999;94:2467–2474.
[11] Kleiner DE, Brunt EM, Van Natta M, Behling C, Contos MJ, Cummings OW, et al. Design and validation of a histological scoring system for nonalcoholic fatty liver disease. Hepatology 2005;41:1313–1321.
[12] Brunt EM, Kleiner DE, Wilson LA, Belt P, Neuschwander-Tetri BA. Nonalcoholic fatty liver disease (NAFLD) activity score and the histopathologic diagnosis in NAFLD: distinct clinicopathologic meanings. Hepatology 2011;53:810–820.
[13] Katz A, Nambi SS, Mather K, Baron AD, Follmann DA, Sullivan G, et al. Quantitative insulin sensitivity check index: a simple, accurate method for assessing insulin sensitivity in humans. J Clin Endocrinol Metab 2000;85:2402–2410.
[14] Smyth GK, Speed T. Normalization of cDNA microarray data. Methods 2003;31:265–273.
[15] Carey VJ, Gentry J, Whalen E, Gentleman R. Network structures and algorithms in bioconductor. Bioinformatics 2005;21:135–136.
[16] Tusher VG, Tibshirani R, Chu G. Significance analysis of microarrays applied to the ionizing radiation response. Proc Natl Acad Sci USA 2001;98:5116–5121.
[17] Henegar C, Tordjman J, Achard V, Lacasa D, Cremer I, Guerre-Millo M, et al. Adipose tissue transcriptomic signature highlights the pathological relevance of extracellular matrix in human obesity. Genome Biol 2008;9:R14.
[18] Prifti E, Zucker JD, Clement K, Henegar C. FunNet: an integrative tool for exploring transcriptional interactions. Bioinformatics 2008;24:2636–2638.
[19] Zhang B, Horvath S. A general framework for weighted gene co-expression network analysis. Stat Appl Genet Mol Biol 2005;4. Article 17.
[20] Emanuelsson O, Brunak S, von Heijne G, Nielsen H. Locating proteins in the cell using TargetP, SignalP and related tools. Nat Protoc 2007;2:953–971.
[21] Bendtsen JD, Jensen LJ, Blom N, Von Heijne G, Brunak S. Feature-based prediction of non-classical and leaderless protein secretion. Protein Eng Des Sel 2004;17:349–356.
[22] Anderson NL, Polanski M, Pieper R, Gatlin T, Tirumalai RS, Conrads TP, et al. The human plasma proteome: a nonredundant list developed by combination of four separate sources. Mol Cell Proteomics 2004;3:311–326.
[23] Nishimura S, Manabe I, Nagasaki M, Eto K, Yamashita H, Ohsugi M, et al. CD8+ effector T cells contribute to macrophage recruitment and adipose tissue inflammation in obesity. Nat Med 2009;15:914–920.
[24] Liu J, Divoux A, Sun J, Zhang J, Clement K, Glickman JN, et al. Genetic deficiency and pharmacological stabilization of mast cells reduce diet-induced obesity and diabetes in mice. Nat Med 2009;15:940–945.
[25] Di Gregorio GB, Yao-Borengasser A, Rasouli N, Varma V, Lu T, Miles LM, et al. Expression of CD68 and macrophage chemoattractant protein-1 genes in human adipose and muscle tissues: association with cytokine expression, insulin resistance, and reduction by pioglitazone. Diabetes 2005;54:2305–2313.
[26] Makkonen J, Westerbacka J, Kolak M, Sutinen J, Corner A, Hamsten A, et al. Increased expression of the macrophage markers and of 11beta-HSD-1 in subcutaneous adipose tissue, but not in cultured monocyte-derived macrophages, is associated with liver fat in human obesity. Int J Obes (Lond) 2007;31:1617–1625.
[27] Apovian CM, Bigornia S, Mott M, Meyers MR, Ulloor J, Gagua M, et al. Adipose macrophage infiltration is associated with insulin resistance and vascular endothelial dysfunction in obese subjects. Arterioscler Thromb Vasc Biol 2008;28:1654–1659.
[28] Cancello R, Henegar C, Viguerie N, Taleb S, Poitou C, Rouault C, et al. Reduction of macrophage infiltration and chemoattractant gene expression changes in white adipose tissue of morbidly obese subjects after surgery-induced weight loss. Diabetes 2005;54:2277–2286.
[29] Tordjman J, Poitou C, Hugol D, Bouillot JL, Basdevant A, Bedossa P, et al. Association between omental adipose tissue macrophages and liver histopathology in morbid obesity: influence of glycemic status. J Hepatol 2009;51:354–362.
[30] Cancello R, Taleb S, Poitou C, Tordjman J, Lacasa D, Guerre-Millo M, et al. Is obesity an inflammatory disease?. Journ Annu Diabetol Hotel Dieu 2006:115–128.
[31] Fontana L, Eagon JC, Trujillo ME, Scherer PE, Klein S. Visceral fat adipokine secretion is associated with systemic inflammation in obese humans. Diabetes 2007;56:1010–1013.
[32] Cancello R, Rouault C, Guilhem G, Bedel JF, Poitou C, Di Blasio AM, et al. Urokinase plasminogen activator receptor in adipose tissue macrophages of morbidly obese subjects. Obes Facts 2011;4:17–25.
[33] Ghosh AK, Vaughan DE. PAI-1 in tissue fibrosis. J Cell Physiol 2011;227:493–507.
[34] Liu W, Xu G, Ma J, Jia W, Li J, Chen K, et al. Osteopontin as a key mediator for vasculogenic mimicry in hepatocellular carcinoma. Tohoku J Exp Med 2011;224:29–39.